

Tightening the Approximation Error of Adversarial Risk with Auto Loss Function Search

Pengfei Xia, Ziqiang Li, and Bin Li, *Member, IEEE*

Abstract—Numerous studies have demonstrated that deep neural networks are easily misled by adversarial examples. Effectively evaluating the adversarial robustness of a model is important for its deployment in practical applications. Currently, a common type of evaluation is to approximate the adversarial risk of a model as a robustness indicator by constructing malicious instances and executing attacks. Unfortunately, there is an error (gap) between the approximate value and the true value. Previous studies manually design attack methods to achieve a smaller error, which is inefficient and may miss a better solution. In this paper, we establish the tightening of the approximation error as an optimization problem and try to solve it with an algorithm. More specifically, we first analyze that replacing the non-convex and discontinuous 0-1 loss with a surrogate loss, a necessary compromise in calculating the approximation, is one of the main reasons for the error. Then we propose AutoLoss-AR, the first method for searching loss functions for tightening the approximation error of adversarial risk. Extensive experiments are conducted in multiple settings. The results demonstrate the effectiveness of the proposed method: the best-discovered loss functions outperform the handcrafted baseline by 0.9%-2.9% and 0.7%-2.0% on MNIST and CIFAR-10, respectively. Besides, we also verify that the searched losses can be transferred to other settings and explore why they are better than the baseline by visualizing the local loss landscape.

Index Terms—Deep Neural Networks, Adversarial Examples, Adversarial Risk, Approximation Error, Loss Function Search.

I. INTRODUCTION

WITH the successful application of deep learning to security-sensitive scenarios, e.g., autonomous driving [1] and biometric identification [2], adversarial robustness becomes increasingly crucial to Deep Neural Networks (DNNs). Unfortunately, numerous studies have shown that unfortified DNNs can be easily fooled by perturbing clean data with imperceptible perturbations [3], [4], [5], which undoubtedly increases the risk of DNN-based systems to malicious attacks. Therefore, to help developers understand the model and build an effective defense, it is necessary to properly evaluate the adversarial robustness before the formal deployment.

Various methods have been proposed over the last few years [6], [7], [8], [9] to evaluate the adversarial robustness of DNNs. One of the most practical methods [4], [10], [11] is to approximate the adversarial risk of the subjected model f as a robustness indicator, i.e.,

$$R(f, D, B, \epsilon) = \mathbb{E}_{(x,y) \sim D} \left[\max_{x' \in B(x, \epsilon)} \ell_{0-1}(f(x'), y) \right], \quad (1)$$

where $(x, y) \sim D$ denote the input data and its ground-truth label sampled from a joint distribution D , $B(x, \epsilon)$ denotes a perceptually similar set with a hyper-parameter ϵ , e.g., within a l_p -norm ball $\|x' - x\|_p \leq \epsilon$, and ℓ_{0-1} denotes the 0-1 loss function.

From the above formula, R reflects the worst-case risk of f under D , B , and ϵ , and is a solid indicator of adversarial robustness. However, accurately computing the true adversarial risk is impractical. There are two reasons for this occurring. The first one is that optimizing the non-convex and discontinuous 0-1 loss is computationally intractable [12]. The other is that the solution to the inner maximization is usually carried out in a high-dimensional and it is difficult to obtain the global optimum. More details will be described in Section III.

To be computationally feasible, two compromises have to be made, that is, replace the 0-1 loss with a surrogate function and employ a specific algorithm to solve the maximization problem. Different surrogates and algorithms establish different attacks and obtain various approximations of the true adversarial risk. For example, Madry et al. [10] utilized the cross-entropy loss and the project gradient descent to generate adversarial examples to evaluate a model. Alzantot et al. [13] proposed a black-box attack by using the output scores as the surrogate and solving the problem with genetic algorithm.

A. Motivation

Unfortunately, there is an error (gap) between an approximation and the true adversarial risk. Such error is often used to compare different attacks: researchers have proposed various techniques to obtain a lower value so that the adversarial robustness of DNNs can be assessed more accurately. However, the manual design of attacks is inefficient and may miss a better solution. Since it depends on the surrogate loss and the algorithm, we wonder that whether the approximation error can be tighten by defining and solving an optimization problem with the above two factors as independent variables. We mainly focus on the loss function part in this paper and leave the algorithm part for future work.

B. Contribution

The main contributions of this paper are as follows.

- We analyze that replacing the non-convex and discontinuous 0-1 loss with a surrogate function, a necessary compromise in calculating the approximation, is one of the two reasons for the error. The choice of surrogate is then formulated as an optimization problem, which can be solved with an algorithm rather than manual design.

- We propose AutoLoss-AR, the first method for searching loss functions for tightening the approximation error of adversarial risk. Each function is coded into a tree and the genetic programming (GP) [14] is adopted for finding a suitable expression in a well-designed space.
- Extensive experiments on multiple datasets, networks structures, training methods, and perceptually similar sets are conducted to test the proposed method. The results consistently demonstrate that AutoLoss-AR is effective in tightening the approximation error. In all experimental settings, a better surrogate than the handcraft baseline can be found. Besides, we verify that the searched losses can be transferred to other settings and explore why they are better than the baseline by visualizing the local loss landscape.

C. Organization

The rest of this paper is organized as follows. The next section briefly reviews related work. In Section III, we detail the approximation error of adversarial risk and formulate the problem. The proposed AutoLoss-AR is introduced in Section IV. Our experimental settings and results are depicted in Section V. We demonstrate the conclusion of this paper in Section VI.

II. RELATED WORK

A. Adversarial Examples

By adding almost imperceptible perturbations on clean input data, adversarial examples can mislead DNNs with high confidence. Such examples are first noticed by Szegedy et al. [3] and have attracted a lot of attention. Goodfellow et al. [4] believed that the existence of adversarial instances is because of the linear nature of neural networks and proposed a single-step attack named the Fast Gradient Sign Method (FGSM) to construct adversaries. Some works [15], [10], [11] have been carried out to extend the single-step attack to multi-step iterations. Among them, the Project Gradient Descent (PGD) attack proposed by Madry et al. [10] is the most typical one and shows a strong attack capability. Carlini and Wagner [6] developed a class of powerful target attacks, C&W attacks, by transforming the constrained problem to the unconstrained one with a penalty. Su et al. [16] designed the one-pixel attack and demonstrated that DNNs can be fooled by only modifying one pixel in the input image.

One of the primary principles for constructing adversaries is that instances with or without perturbations should be perceptually similar to humans. The forenamed methods mostly conform to this by limiting the l_p -norm of the difference between the clean data and its adversary to a small value. There are some others that maintain high perceptual similarity without the l_p -norm limitation [17], [18], [19], [20], [21]. For example, Engstrom et al. [19] found that neural networks are vulnerable to simple image transformations, such as rotation and translation. Xiao et al. [21] proposed to construct adversaries by slightly flowing the position of each pixel in the input image.

No matter what method is used to construct adversarial examples, these attacks evaluate the robustness of a model by computing an approximation of the true adversarial risk, which introduces an error.

B. Adversarial Training

To improve the adversarial robustness of DNNs, many defenses have been come into the scene, e.g., data preprocessing [22], [23], feature squeezing [24], and gradient regularization [25], [26]. Among them, the most intuitive and empirically effective one is reusing adversarial examples as augmented data to train DNNs, i.e., Adversarial Training (AT). This kind of method is first introduced by Goodfellow et al. [4]. Madry et al. [10] developed it by training deep models with stronger adversaries generated by PGD. Subsequent works mainly focus on accelerating training [27], [28] and improving the resistance [29], [30], [31]. Zhang et al. [32] characterized the trade-off between accuracy and robustness and proposed TRADES, which optimizes a regularized surrogate loss to improve the adversarial robustness of DNNs. Wang and Zhang [31] proposed the Bilateral Adversarial Training (BAT), where both the data and the label are perturbed. Tramer and Boneh [30] developed the Multiple Perturbation Adversarial Training (MPAT) to defense multiple types of attacks simultaneously.

In this paper, our experiments are performed on both standard training and adversarial training models.

C. Robustness Evaluation

Effectively evaluating the adversarial robustness of DNNs is an important issue for both academic research and practical applications. Most of the previous evaluations can be divided into two groups: attack-based methods [4], [6], [10], [11] and bound-based methods [7], [33], [8], [34], [9]. Attack-based evaluations, such as FGSM [4] and PGD [10], directly generate adversarial examples to attack deep models to assess the worst-case risk, i.e., adversarial risk, as a robustness indicator. Hendrycks and Dietterich [35] introduced widely used visual corruptions and adversarial perturbations to generate two datasets for benchmarking DNNs' robustness. Bound-based methods try to provide a fundamental bound, or its estimation, for analyzing the robustness of classifiers to adversarial examples. Weng et al. [8] proposed a metric named the Cross-Lipschitz extreme value for network robustness (CLEVER) to measure the robustness without any attack. Weng et al. [34] provided efficient algorithms, i.e., Fast-Lin and Fast-Lip, for computing a certified lower bound by exploiting the ReLU property. Zhang et al. [9] extended it to some other activation functions that are not piece-wise linear. Both of the above two types have their own strengths and weaknesses. For example, attack-based methods are computationally efficient, but there is a possibility of providing a false sense of security [36], [37]. Bound-based ones provide certified results, but may be limited to a special type of network.

This paper focus on attack-based evaluations. A more reasonable attack can lead to a more accurate evaluation of adversarial robustness. We do not design manually, but formulate the problem of tightening the approximation error and try to solve it from the perspective of optimization.

D. Auto Loss Function Search

Auto loss function search, which belongs to AutoML [38], [39], has raised the interest of researchers in recent years. At present, all studies concentrate on how to find a loss function to train a model with a better performance. For example, Li et al. [40] and Wang et al. [41] proposed to optimize loss functions for face recognition, where the search is performed on specific hyper-parameters in the fixed formulas. Subsequently, Li et al. [42] and Liu et al. [43] introduced this idea into semantic segmentation and object detection, respectively. More recently, Li et al. [44] proposed AutoLoss-Zero, a general framework for learning tasks. They verified the effectiveness of AutoLoss-Zero on four tasks, i.e., semantic segmentation, object detection, instance segmentation, and pose estimation.

We utilize this idea to tighten the approximation error of adversarial risk, a task different from the previous learning ones. Therefore, this requires us to better fit the adversarial robustness evaluation task when designing the search space of the loss function.

III. PROBLEM FORMULATION

A. Approximation Error

As formulated in Equation 1, R ideally reflects the worst-case risk of the model f under D , B , and ϵ , and is a good indicator of adversarial robustness. Unfortunately, it is hard to compute the true adversarial risk accurately. Two compromises have to be made to get an estimation of R , which introduce the approximation error.

The first one is about the loss function. As is well known, optimizing the non-convex and discontinuous 0-1 loss is computationally intractable [12]. So the common practice is to maximize a surrogate loss function, that is,

$$R'(f, D, B, \epsilon, \ell_s) = \mathbb{E}_{(x,y) \sim D} [\ell_{0-1}(f(x'), y)], \quad (2)$$

subject to $x' = \operatorname{argmax}_{x' \in B(x, \epsilon)} \ell_s(f(x'), y)$

where ℓ_s denotes a surrogate, such as the cross-entropy loss.

An important issue is that can the point x' that maximizes ℓ_s also maximizes ℓ_{0-1} . If the answer is positive, then there is no gap between R' and R , i.e., $R' = R$, otherwise $R' < R$. A similar question named surrogate risk consistency has been studied in empirical risk minimization, where Bartlett et al. [45] and Tewari et al. [46] have proved that the optimization is consistent for most common surrogate losses. However, the conclusion cannot be directly transferred to the adversarial risk, because in the adversarial setting, the goal is to find an adversary x' within $B(x, \epsilon)$ to maximize ℓ_s , rather than find optimal weights of f to minimize ℓ_s in the empirical risk setting. On the contrary, we argue that for a multi-class problem, an inappropriate choice makes the consistency cannot be guaranteed. We use a toy example to illustrate it.

Considering a 3-class problem. Given an input $x \in [-1, 1]^2$, suppose a single-layer neural network with softmax is used to classify x into three categories $y \in \{0, 1, 2\}$, i.e.,

$$f(x) = \operatorname{softmax} \left(\begin{bmatrix} 0.2 & 0.8 \\ 0.9 & 0.4 \\ 0.3 & 0.9 \end{bmatrix} \cdot \begin{bmatrix} x_0 \\ x_1 \end{bmatrix} \right). \quad (3)$$

What we are interested in is the values of 0-1 loss and surrogate loss. Specifically, we adopt the cross-entropy loss as the proxy and calculate the values of $\ell_{0-1}(f(x), 0)$ and $\ell_s(f(x), 0)$. The results are shown in Figure 1. Obviously, within $B(x, \epsilon)$, x' that maximizes ℓ_s may not maximize ℓ_{0-1} .

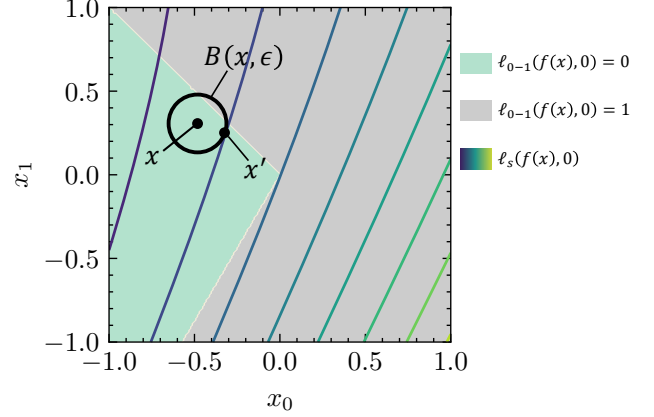


Fig. 1. An example of a 3-class single-layer neural network to illustrate the optimization inconsistency between the 0-1 loss and the surrogate (cross-entropy) loss in the adversarial setting, where x' maximizes ℓ_s , while $\ell_{0-1} = 0$.

The second compromise is about the optimization algorithm. Directly computing R' is still difficult, because a DNN f is a highly nonlinear non-convex function with high-dimensional data as its input. It is usually impossible to get the inner global maximum. We, therefore, have to compromise further: using the gradient descent or other methods to find an approximately optimal solution, that is,

$$R''(f, D, B, \epsilon, \ell_s, m) = \mathbb{E}_{(x,y) \sim D} [\ell_{0-1}(f(x'), y)], \quad (4)$$

subject to $x' = m(f, x, y, B, \epsilon, \ell_s)$

where m denotes a specific algorithm. It is worth noting that the existence of this part has been verified by Uesato et al. [47].

The approximation error can be defined as

$$E(f, D, B, \epsilon, \ell_s, m) = R(f, D, B, \epsilon) - R''(f, D, B, \epsilon, \ell_s, m). \quad (5)$$

B. Optimization Problem

Previous attacks reduce the error E by manually selecting and designing ℓ_s and m to get a closer approximation of the true adversarial risk. In this paper, we treat it as an optimization problem, and the goal is to

$$\begin{aligned} & \min_{\ell_s \in \mathcal{S}, m \in \mathcal{M}} E(f, D, B, \epsilon, \ell_s, m) \\ &= \min_{\ell_s \in \mathcal{S}, m \in \mathcal{M}} R(f, D, B, \epsilon) - R''(f, D, B, \epsilon, \ell_s, m) \end{aligned} \quad (6)$$

where \mathcal{S} and \mathcal{M} denote the space of the surrogate loss and the algorithm, respectively. Since at given f , D , B and ϵ , R is an unknown constant, and $R \geq R''$, optimizing Equation 6 is equivalent to optimizing

$$\max_{\ell_s \in \mathcal{S}, m \in \mathcal{M}} R''(f, D, B, \epsilon, \ell_s, m). \quad (7)$$

In this paper, we focus on the surrogate loss part and fix m to a specific algorithm. Therefore, the goal we try to solve here is

$$\max_{\ell_s \in \mathcal{S}} R''(f, D, B, \epsilon, \ell_s, m). \quad (8)$$

Next, we introduce the method used to deal with the above problem.

IV. METHODOLOGY

A. Overview

To solve the above problem, each loss function is expressed as a tree, and the genetic programming (GP) [14] is adopted for optimizing a suitable solution among the search space. Our method is similar to CSE-AutoLoss [43] and AutoLoss-Zero [44], and is dubbed as AutoLoss-AR, which is the abbreviation of auto loss function search for adversarial risk. The major difference is that AutoLoss-AR focuses on searching for a suitable loss for tightening the approximation error of adversarial risk, rather than training a model for a specific task with a better performance. The overview of the search pipeline is presented in Figure 2, where the search space and the search algorithm are two important parts. More details are described below.

B. Search Space

The search space, which is composed of the input node set and the primitive operation set, determines the set or domain that an algorithm searches. To design a suitable space, we refer to some hand-crafted loss functions in the adversarial setting, including the cross-entropy loss [3], [4], [10], [11], [30], the C&W losses [6], the margin logit loss [47], and other loss functions [13], [48]. Besides these two sets, another factor that affects the search space is the maximum depth md of a tree.

1) *Input Node Set*: We consider evaluating the adversarial robustness of a classification model in this paper. The input node set contains two variables, p and q , and two constants, 0 and 1, where p denotes the logits of the model output $f(x)$ and q denotes the one-hot form of the true label y . p and q are of the same shape $(1, C)$, where C is the number of categories. The purpose of using the logits instead of $f(x)$, and adding two constants, is to expand the search space for a possible solution. Since $f(x) = \text{softmax}(p)$, to ensure that the losses with $f(x)$ as input are easy to explore, we have added Softmax to the primitive operation set.

2) *Primitive Operation Set*: The primitive operations, including element-wise and aggregation operations, are listed in Table I. Since the loss calculation is usually performed on a batch, we define the inputs of each operation to be of shape (N, C) or $(N, 1)$, where N denotes the batch size. For element-wise functions, including Add, Mul, Neg, Abs, Inv, Sqrt, Square, Exp, and Log, the output dimension is the same as the input dimension. The aggregation operations, including Max, Sum, and Softmax, are performed on the second dimension and keep that dimension without reduction. It is worth noting that for each expression coded by a tree, the

output o is a matrix of shape (N, C) or $(N, 1)$, so it needs to be calculated to a real number by some operations, i.e.,

$$\ell_s = \frac{1}{N} \sum_{n=1}^N \sum_{c=1}^{C \text{ or } 1} o_{nc}. \quad (9)$$

A surrogate loss is composed of a tree-encoded expression and fixed aggregation operations in Equation 9.

TABLE I
PRIMITIVE OPERATION SET. THE SHAPE OF x AND y IS (N, C) OR $(N, 1)$, WHERE N DENOTES THE BATCH SIZE, C DENOTES THE NUMBER OF CATEGORIES. γ IS A SMALL VALUE TO AVOID ZERO DIVISION.

Operation	Expression	Arity
Add	$x + y$	2
Mul	$x \times y$	2
Neg	$-x$	1
Abs	$ x $	1
Inv	$\text{sign}(x) / (x + \gamma)$	1
Sqrt	$\text{sign}(x) \cdot \sqrt{ x + \gamma}$	1
Square	x^2	1
Exp	e^x	1
Log	$\text{sign}(x) \cdot \log(x + \gamma)$	1
Max	$\max(x)$	1
Sum	$\text{sum}(x)$	1
Softmax	$\text{softmax}(x)$	1

C. Search Algorithm

We adopt GP, a population-based searching technique, as the algorithm to find a suitable surrogate for tightening the approximation error among the search space. As shown in Figure 2, the search algorithm contains five steps: initialization, evaluation, selection, crossover, and mutation.

1) *Initialization*: At the initialization step, ps loss functions are randomly generated to form the initial population, where ps denotes the size of the population.

2) *Evaluation*: Because the optimization goal is Equation 8, we directly calculate R'' for each expression tree as its fitness, where the value is between 0 and 1. During the evaluation process, the generated expression may be infeasible to compute, such as invalid values NaN, Inf, etc. At this time, we set its fitness to 0. This strategy also saves time to a certain extent.

3) *Selection*: We adopt the tournament [49] as the selection strategy in AutoLoss-AR. It involves holding several tournaments among a few individuals randomly chosen from the population. The winner of each tournament (the one with the largest fitness) is selected for the next step. Two hyper-parameters, namely the size of the tournament ts and the times of selection st , are used to control the entire process.

4) *Crossover and Mutation*: The crossover and mutation steps are used to generate the offspring population. These expression trees randomly perform one-point crossover and mutate independently, where the probabilities of mating and mutation are cp and mp .

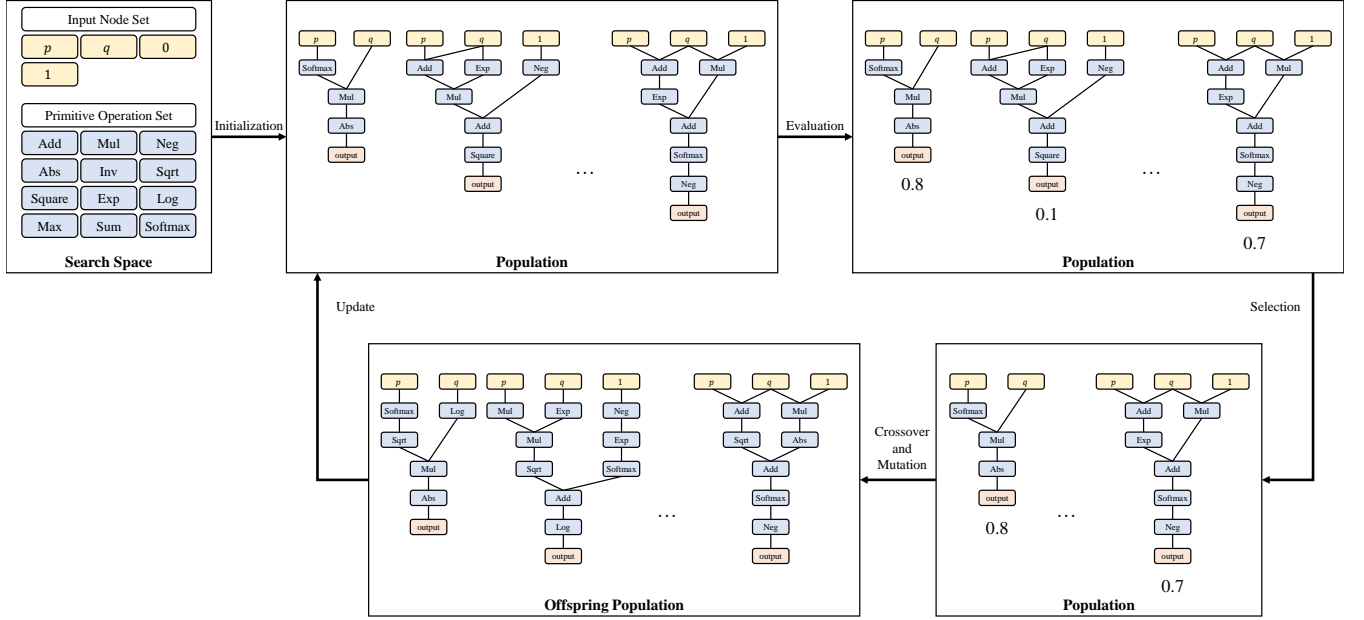


Fig. 2. Overview of the search pipeline of AutoLoss-AR. The search space and the search algorithm are two important parts, where the former is composed of two sets and the latter contains five steps.

V. EXPERIMENTS

A. Purpose

The purpose of our experiments is to answer the following questions:

- Under given conditions, i.e., f , D , B , ϵ , and m , can AutoLoss-AR obtain a better solution than the handcraft loss for tightening the approximation error?
- Can the searched loss function be used in other conditions, such as a different model f or a different dataset D ?
- If the searched surrogate performs better than the handcraft one, then why?

B. Setup

As shown in Equation 8, in addition to the surrogate ℓ_s to be searched, the factors that affect the approximation error E include the test model f , the dataset D , the similar set and its hyper-parameter B and ϵ , and the algorithm of generating adversaries m . To comprehensively test AutoLoss-AR, we consider multiple settings.

1) *Dataset*: Two image classification datasets, MNIST [50] and CIFAR-10 [51], are selected, which are often used in previous studies about adversarial examples [3], [4], [6], [10]. For MNIST, once the surrogate loss is searched, except for the original test set, we also use the extended data [52] for testing.

2) *Network Structure*: For each dataset, two network structures, as shown in Table II, are employed for training tested models f .

3) *Training Method*: We adopt two training methods, standard training (ST) and adversarial training (AT), for each

TABLE II

NETWORK STRUCTURES USED IN THE EXPERIMENTS. CONV(X, Y): A CONVOLUTIONAL LAYER WITH $X \times X$ KERNEL SIZE AND Y OUTPUT CHANNELS. BN: A BATCH NORMALIZATION LAYER [53]. ReLU: A RECTIFIED LINEAR ACTIVATION LAYER. MP(X): A MAX POOLING LAYER WITH $X \times X$ KERNEL SIZE. GAP: A GLOBAL AVERAGE POOLING LAYER [54]. FC(X): A FULLY CONNECTED LAYER WITH X OUTPUT CHANNELS.

MNIST		CIFAR-10	
NET-1	NET-2	NET-1	NET-2
Conv(5, 4)	Conv(3, 8)	Conv(3, 16)	Conv(3, 16)
BN + ReLU	BN + ReLU	BN + ReLU	BN + ReLU
MP(2)	MP(2)	MP(2)	MP(2)
Conv(5, 8)	Conv(3, 16)	Conv(3, 16)	Conv(3, 16)
BN + ReLU	BN + ReLU	BN + ReLU	BN + ReLU
MP(2)	MP(2)	MP(2)	MP(2)
Conv(5, 16)	Conv(3, 32)	Conv(3, 32)	Conv(3, 32)
BN + ReLU	BN + ReLU	BN + ReLU	BN + ReLU
MP(2)	MP(2)	MP(2)	MP(2)
Conv(5, 32)	Conv(3, 64)	Conv(3, 64)	Conv(3, 32)
GAP	GAP	BN + ReLU	BN + ReLU
FC(10)	FC(10)	MP(2)	MP(2)
		Conv(3, 128)	Conv(3, 64)
		BN + ReLU	BN + ReLU
		GAP	Conv(3, 128)
		FC(10)	BN + ReLU
			GAP
			FC(10)

network structure. ST follows the principle of empirical risk minimization, that is,

$$f = \operatorname{argmin}_{f \in \mathcal{F}} \mathbb{E}_{(x,y) \sim D} [\ell_{ce}(f(x), y)], \quad (10)$$

where \mathcal{F} denotes the space determined by the structure and ℓ_{ce} denotes the cross-entropy loss. AT optimizes parameters through the formula

$$f = \operatorname{argmin}_{f \in \mathcal{F}} \mathbb{E}_{(x,y) \sim D} \left[\max_{x' \in B(x, \epsilon)} \ell_{ce}(f(x'), y) \right]. \quad (11)$$

TABLE III
 ϵ SETTINGS UNDER DIFFERENT f , D , AND B .

$B \backslash D, f$	MNIST				CIFAR-10			
	NET-1, ST	NET-2, ST	NET-1, AT	NET-2, AT	NET-1, ST	NET-2, ST	NET-1, AT	NET-2, AT
l_∞	0.07	0.07	0.28	0.24	0.005	0.005	0.024	0.024
l_1	25.0	25.0	34.0	36.0	7.4	7.4	34.0	34.0
l_2	1.3	1.4	5.1	5.6	0.19	0.18	0.9	0.9

Specifically, as suggested in [10], we use PGD with 7 steps and l_∞ -norm to training models, where ϵ is set to 0.1 and 0.01 for MNIST and CIFAR-10, respectively. It should be noted that these hyper-parameter settings are only used in AT.

4) *Similar Set*: We consider limiting the adversary to be within the l_p -norm sphere of the clean sample to ensure the perceptual similarity, i.e., $\|x' - x\|_p \leq \epsilon$, where $p = \infty$, $p = 1$, and $p = 2$. The setting of ϵ is determined according to the specific f , D , and B , so that the approximation of adversarial risk is about 0.7. These values are shown in Table III.

5) *Algorithm*: PGD with 10 steps (PGD-10) is used as the algorithm m to generate adversarial examples during AutoLoss-AR's search. Once the search is completed, the found loss function will be also examined on PGD with 100 steps (PGD-100).

6) *Handcraft Baseline*: The cross-entropy (CE) loss is used as a baseline, which is widely used in many attacks [3], [4], [10], [11], [30].

7) *Hyper-parameters in AutoLoss-AR*: Hyper-parameter settings in AutoLoss-AR are shown in Table IV.

TABLE IV
 HYPER-PARAMETER SETTINGS IN AUTOLOSS-AR.

Hyper-parameter	Description	Value
gn	Number of the generation	100
md	Maximum depth of the tree	25
ps	Size of the population	200
ts	Size of the tournament	3
st	Times of the selection	200
cp	Probability of the crossover	0.5
mp	Probability of the mutation	0.3

8) *Implement Details*: For all models that need to be trained, we adopt the stochastic gradient descent (SGD) with momentum of 0.9 and weight decay of $5e-4$ as the optimizer. The batch size is set to 1024 for MNIST and 512 for CIFAR-10. The initial learning rate is set to 0.01 and is dropped by 10 after 80 and 120 epochs. All images are normalized to [0-1]. Our experiments are implemented with PyTorch [55] and DEAP [56], and run on an NVIDIA Tesla V100 GPU.

C. Results

1) *Question 1*: Under given f , D , B , ϵ , and m , can AutoLoss-AR obtain a better solution than the handcraft baseline for tightening the approximation error? To answer this question, we use the proposed method to find surrogate losses in multiple settings. For each setting, the search process runs independently 20 times, and the statistical results for MNIST and CIFAR-10 are shown in Figure 3 and Figure 4.

For MNIST, the best-discovered loss functions outperform the baseline by 1.8%, 2.9%, 2.1% for NET-1, ST, 1.1%, 0.9%, 0.9% for NET-2, ST, 1.8%, 1.2%, 1.0% for NET-1, AT, and 2.9%, 0.9%, 0.9% for NET-2, AT, with l_∞ , l_1 and l_2 limitations, respectively. The values for CIFAR-10 are 0.7%, 1.1%, 1.0% for NET-1, ST, 1.1%, 1.1%, 1.1% for NET-2, ST, 2.0%, 1.9%, 1.9% for NET-1, AT, and 1.9%, 1.9%, 1.8% for NET-2, AT, with l_∞ , l_1 and l_2 limitations, respectively. Besides, the success rate of searching for losses exceeding the baseline is 100%. These results all demonstrate that the answer to Question 1 is: yes, AutoLoss-AR is able to obtain a better surrogate than the manual design loss for a closer approximation of the adversarial risk.

2) *Question 2*: Can the searched loss function be used in other conditions? The best-discovered loss in one setting is tested in other settings to answer this question.

First of all, we keep f , D , and B unchanged, and change ϵ and m . The results are shown in Figure 5 and Figure 6. It shows that the losses found by using PGD-10 as the adversaries generation algorithm can be applicable to PGD-100. Compared with PGD-10, more iterations get closer evaluation values. But it will not change that using the searched loss to evaluate is better than using the CE loss. In terms of ϵ , for MNIST, in some cases, reducing ϵ leads to a reduction in the improvement of the searched loss, which does not appear on CIFAR-10.

Second, we consider different data D and keep the other factors unchanged. The results, which are shown in Figure 7, demonstrate that the searched losses can maintain the effect on the extended test set.

Last, we cross-test the effects under different f and B , as shown in Figure 8. For CIFAR-10, except for using NET-2, AT, the other searched losses can be applied to all settings. Besides, when evaluating the models trained with AT, using the searched loss seems to have a greater improvement to the CE loss. We argue this is because there is a process of maximizing the CE loss in AT, which leads to a certain overfit of the trained models against attacks that use this loss. The results on MNIST are more complicated. Except for the diagonal, the brightness of other areas is irregular. But most of them are effective. The possible reason for the different results of MNIST and CIFAR-10 will be discussed in Question 3.

In summary, the answer to Question 2 is: mostly, but there are cases, when some conditions change, the improvement by the searched losses cannot be maintained.

3) *Question 3*: If the searched surrogate performs better than the handcraft one, then why? To answer this question, we record each step of PGD-100 in using the CE loss and the

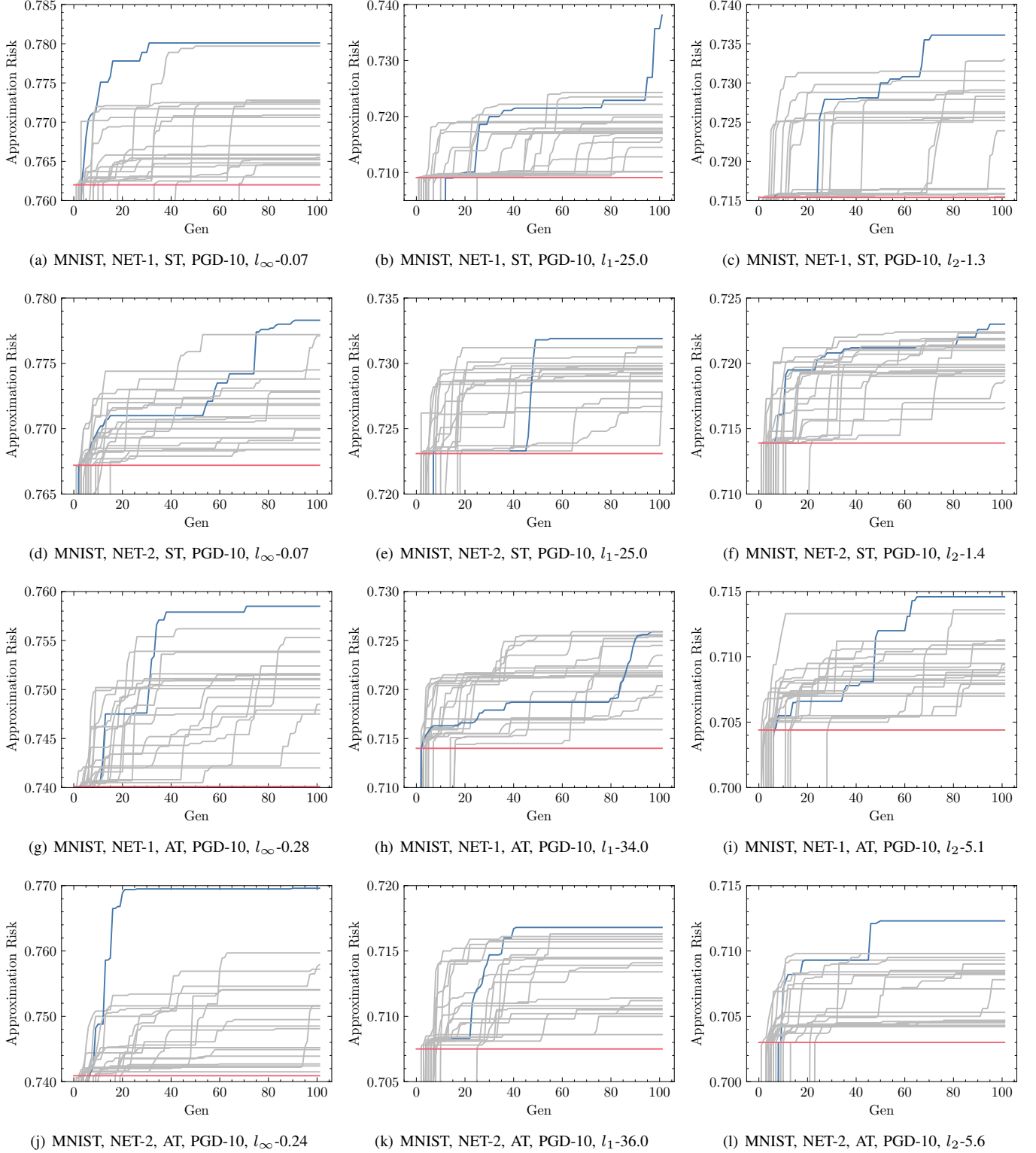


Fig. 3. 20 statistical results on MNIST. The red line represents the baseline, the blue line represents the run with the best searched surrogate, and the gray lines represent the other 19 runs.

searched losses respectively, and use these as two directions to visualize the local loss landscape, as shown in Figure 9.

The results indicate that there may be two reasons. The first one is the specific algorithm m , such as PGD-10 used in this paper, cannot guarantee to find the global optimum, although

the CE loss has good local consistency with the 0-1 loss. The searched surrogate is easier for the algorithm to find a more suitable adversary. For example, as shown in Figure 9(c), the value of the CE loss is obviously greater along the x-axis than along the y-axis, but PGD-100 finally chose the y-axis

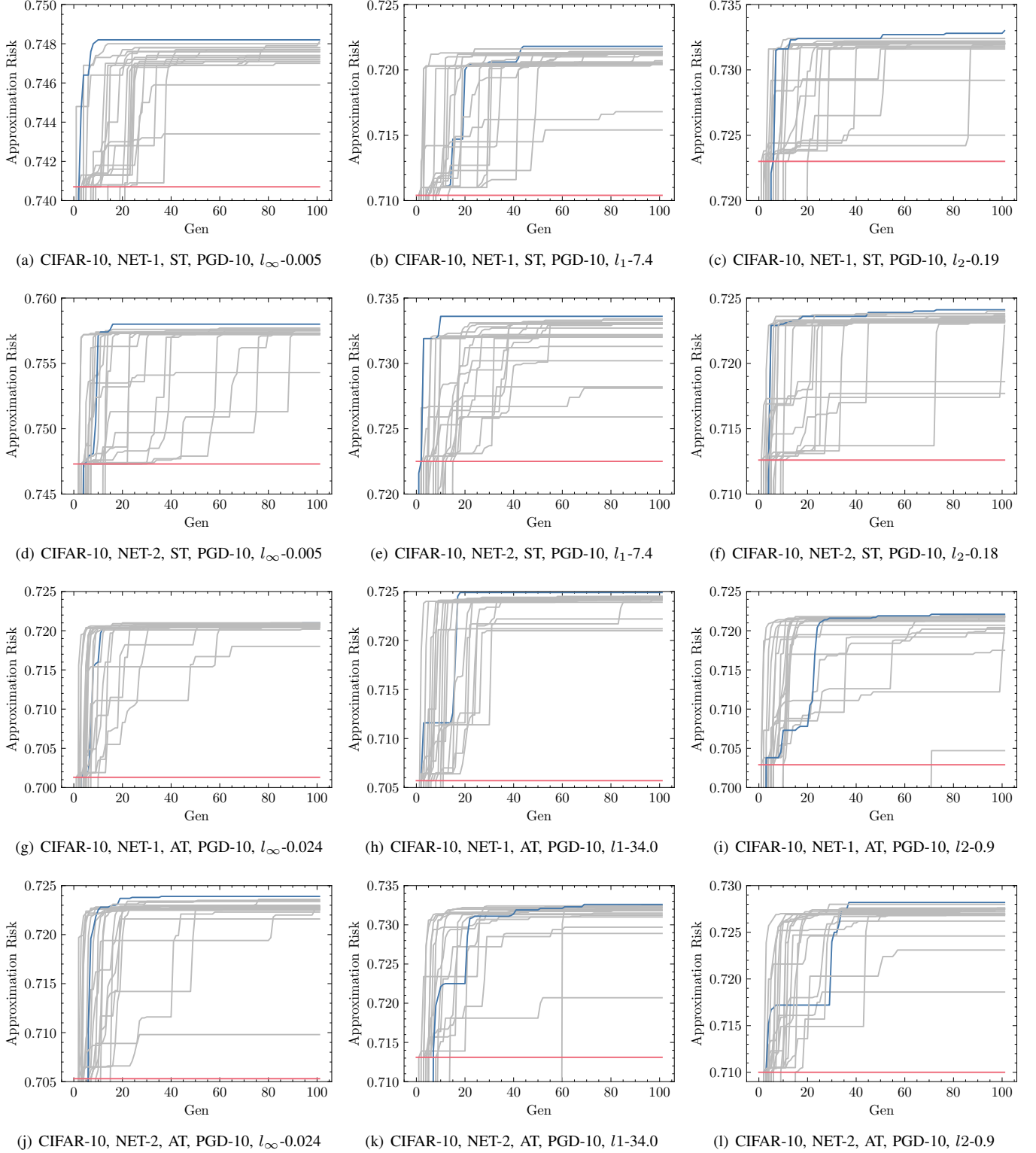


Fig. 4. 20 statistical results on CIFAR-10. The red line represents the baseline, the blue line represents the run with the best searched surrogate, and the gray lines represent the other 19 runs.

direction. Most of the results of MNIST are for this reason.

The second one is the local consistency between the searched loss and the 0-1 loss is better than the CE loss. For example, as shown in Figure 9(l), maximizing the CE loss does not maximize the 0-1 loss. Most of the results of CIFAR-10

are for this reason. Because the main reasons that the searched loss is better than the baseline on the two datasets are different, it partially explains the different results in Figure 8.

So the answer is: two reason, one is the algorithm m and the searched losses are more matched and the other is local

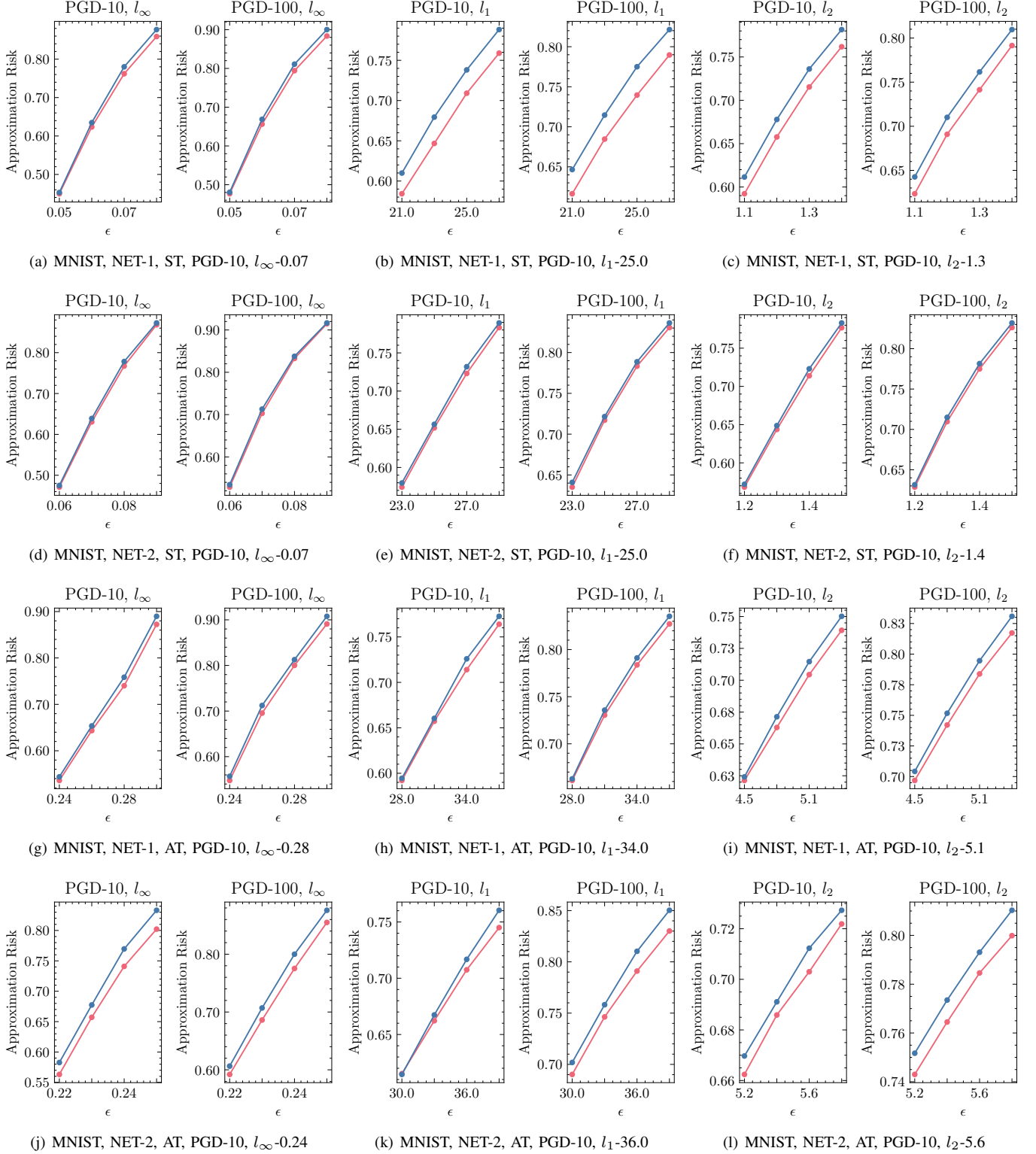


Fig. 5. Results with different ϵ and m on MNIST. The red line represents the baseline and the blue line represents the best searched surrogate.

consistency between the searched loss and the 0-1 loss is better, which are also in line with our analysis in Section III.

4) *Qualitative Examples:* Some qualitative examples are shown in Figure 10, where both adversaries are visually similar to clean images.

VI. CONCLUSION

We establish the tightening of the approximation error as an optimization problem and solve it with an algorithm. Specifically, we focus on the choice of surrogate loss, which is one of the two factors that affect the error, and propose

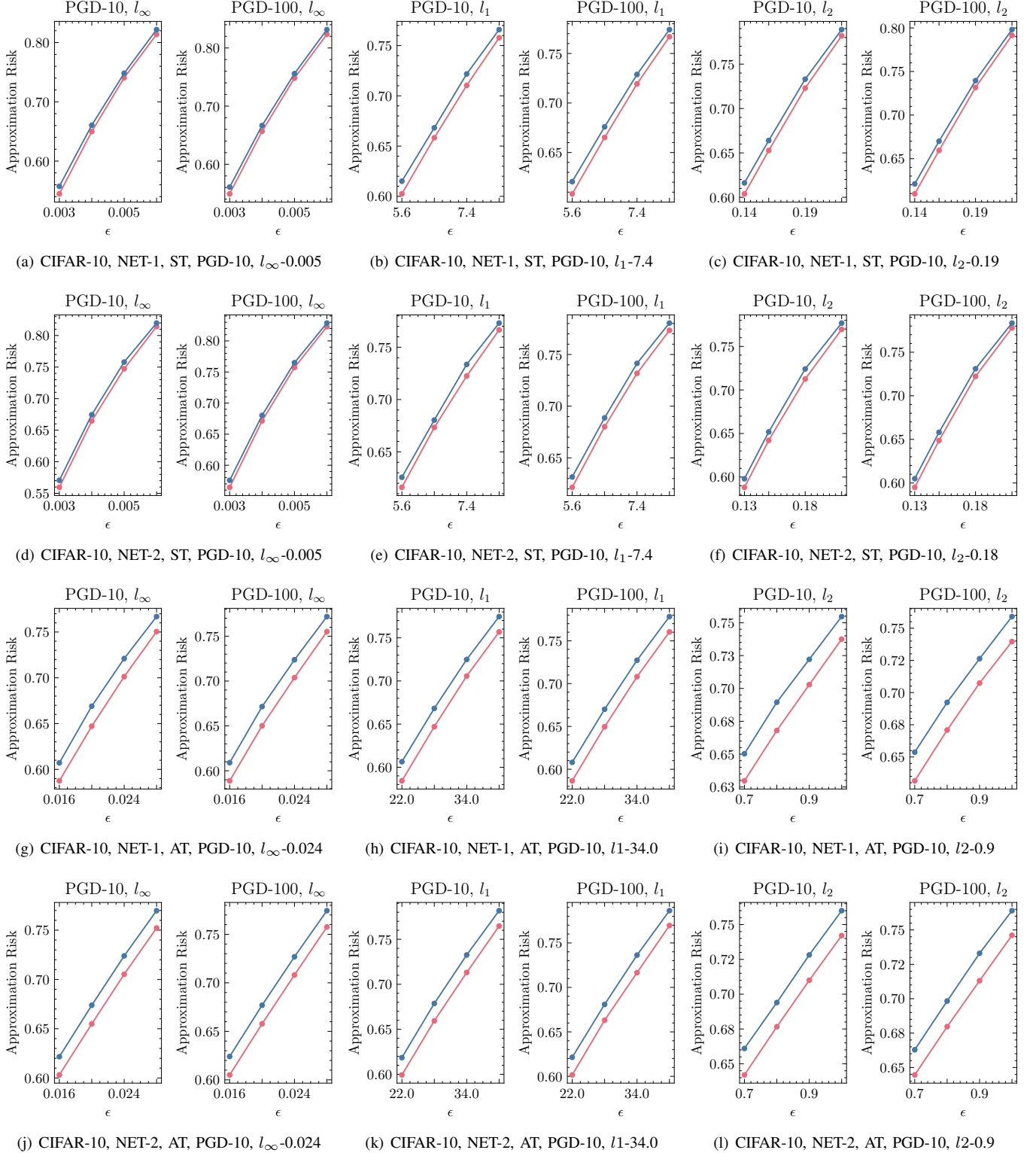


Fig. 6. Results with different ϵ and m on CIFAR-10. The red line represents the baseline and the blue line represents the best searched surrogate.

AutoLoss-AR to find a possible solution with tree coding and GP algorithm. Experiments are conducted on MNIST and CIFAR-10 in multiple settings to verify the effectiveness of the proposed method. The results show that the best-discovered loss functions outperform the handcrafted baseline by 0.9%-2.9% and 0.7%-2.0% on these two datasets, respectively. In

some settings, the searched losses are transferable. Besides, we also identify two reasons why the searched loss is better than the baseline by visualizing the local loss landscape: (1) the searched loss is easier to optimize to find a deceptive adversary and (2) the local consistency between the searched loss and the 0-1 loss is better.

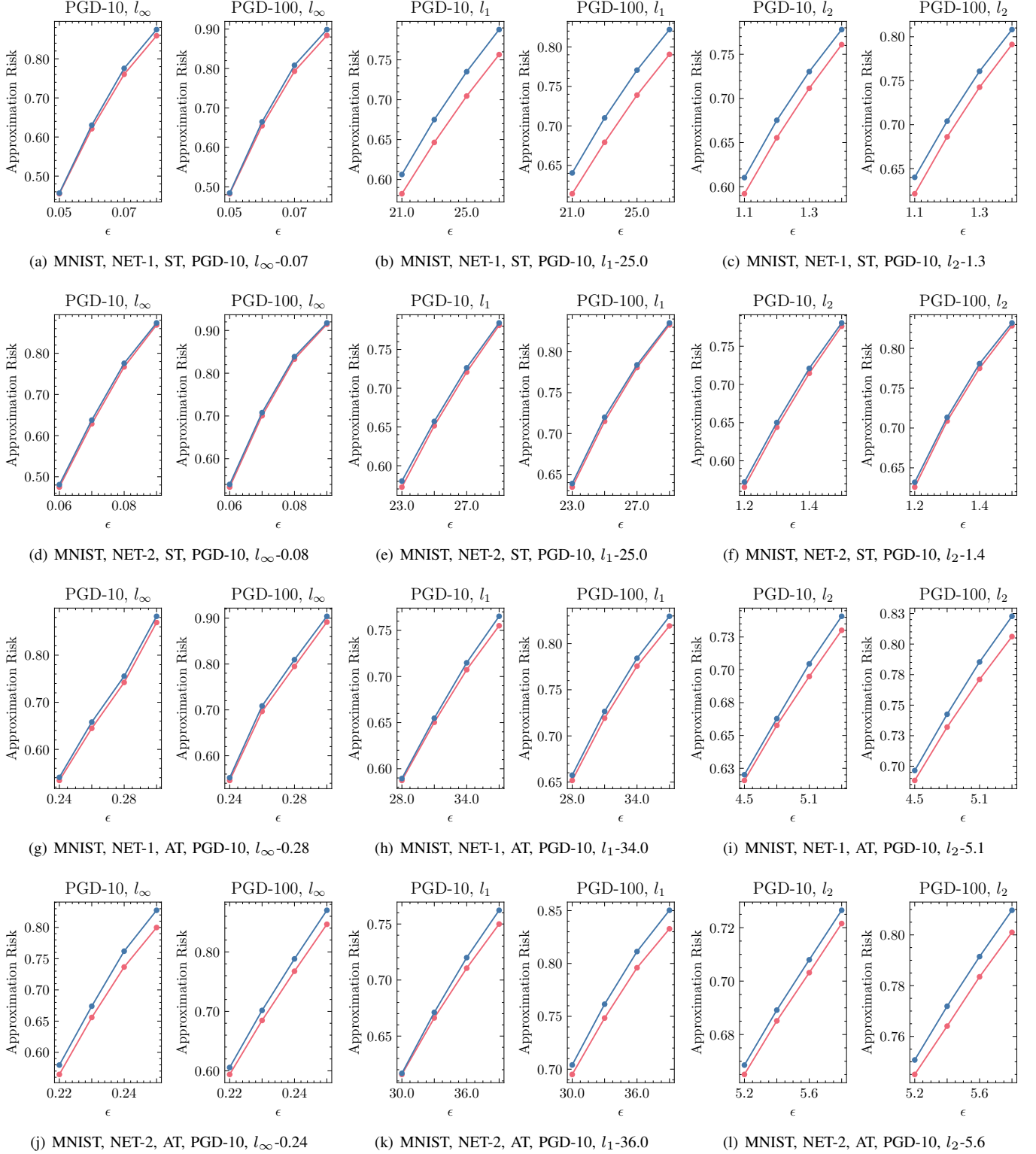


Fig. 7. Results with different D on MNIST. The red line represents the baseline and the blue line represents the best searched surrogate.

ACKNOWLEDGMENT

The work is partially supported by the National Natural Science Foundation of China under grand No.U19B2044 and No.61836011.

REFERENCES

- [1] S. Grigorescu, B. Trasnea, T. Cocias, and G. Macesanu, "A survey of deep learning techniques for autonomous driving," *Journal of Field Robotics*, vol. 37, no. 3, pp. 362–386, 2020.
- [2] K. Sundararajan and D. L. Woodard, "Deep learning for biometrics: A survey," *ACM Computing Surveys (CSUR)*, vol. 51, no. 3, pp. 1–34, 2018.

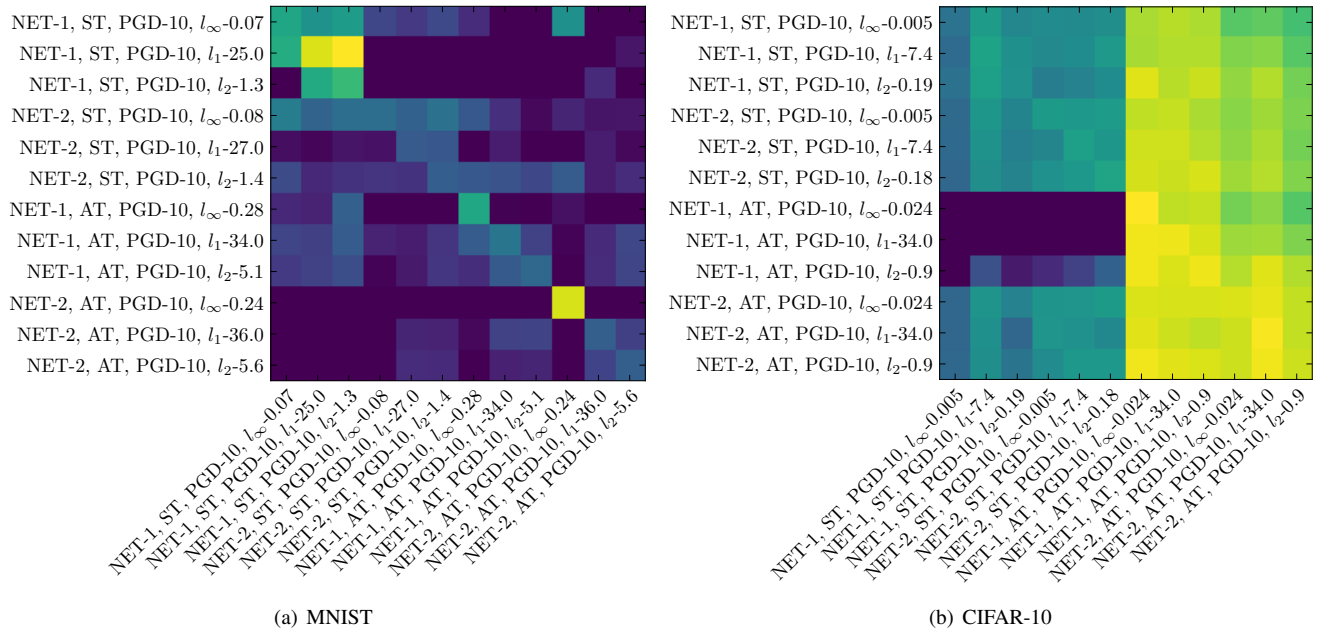


Fig. 8. Results with different f and B on MNIST and CIFAR-10. The vertical axis represents the settings used during the search, and the horizontal axis represents the settings used during the test. The color represents the improvement of the search losses to the baseline, the brighter, the greater. Dark blue means no or negative improvement.

- [3] C. Szegedy, W. Zaremba, I. Sutskever, J. Bruna, D. Erhan, I. Goodfellow, and R. Fergus, "Intriguing properties of neural networks," *arXiv preprint arXiv:1312.6199*, 2013.
- [4] I. J. Goodfellow, J. Shlens, and C. Szegedy, "Explaining and harnessing adversarial examples," *arXiv preprint arXiv:1412.6572*, 2014.
- [5] S.-M. Moosavi-Dezfooli, A. Fawzi, and P. Frossard, "Deepfool: a simple and accurate method to fool deep neural networks," in *Proceedings of the IEEE conference on computer vision and pattern recognition*, 2016, pp. 2574–2582.
- [6] N. Carlini and D. Wagner, "Towards evaluating the robustness of neural networks," in *2017 IEEE Symposium on Security and Privacy (SP)*. IEEE, 2017, pp. 39–57.
- [7] M. Hein and M. Andriushchenko, "Formal guarantees on the robustness of a classifier against adversarial manipulation," *arXiv preprint arXiv:1705.08475*, 2017.
- [8] T.-W. Weng, H. Zhang, P.-Y. Chen, J. Yi, D. Su, Y. Gao, C.-J. Hsieh, and L. Daniel, "Evaluating the robustness of neural networks: An extreme value theory approach," *arXiv preprint arXiv:1801.10578*, 2018.
- [9] H. Zhang, T.-W. Weng, P.-Y. Chen, C.-J. Hsieh, and L. Daniel, "Efficient neural network robustness certification with general activation functions," *arXiv preprint arXiv:1811.00866*, 2018.
- [10] A. Madry, A. Makelov, L. Schmidt, D. Tsipras, and A. Vladu, "Towards deep learning models resistant to adversarial attacks," *arXiv preprint arXiv:1706.06083*, 2017.
- [11] Y. Dong, F. Liao, T. Pang, H. Su, J. Zhu, X. Hu, and J. Li, "Boosting adversarial attacks with momentum," in *Proceedings of the IEEE conference on computer vision and pattern recognition*, 2018, pp. 9185–9193.
- [12] S. Arora, L. Babai, J. Stern, and Z. Sweedyk, "The hardness of approximate optima in lattices, codes, and systems of linear equations," *Journal of Computer and System Sciences*, vol. 54, no. 2, pp. 317–331, 1997.
- [13] M. Alzantot, Y. Sharma, S. Chakraborty, H. Zhang, C.-J. Hsieh, and M. B. Srivastava, "Genattack: Practical black-box attacks with gradient-free optimization," in *Proceedings of the Genetic and Evolutionary Computation Conference*, 2019, pp. 1111–1119.
- [14] J. R. Koza, *Genetic programming: on the programming of computers by means of natural selection*. MIT press, 1992, vol. 1.
- [15] A. Kurakin, I. Goodfellow, and S. Bengio, "Adversarial machine learning at scale," *arXiv preprint arXiv:1611.01236*, 2016.
- [16] J. Su, D. V. Vargas, and K. Sakurai, "One pixel attack for fooling deep neural networks," *IEEE Transactions on Evolutionary Computation*, vol. 23, no. 5, pp. 828–841, 2019.
- [17] M. Sharif, S. Bhagavatula, L. Bauer, and M. K. Reiter, "Accessorize to a crime: Real and stealthy attacks on state-of-the-art face recognition," in *Proceedings of the 2016 ACM SIGSAC conference on computer and communications security*, 2016, pp. 1528–1540.
- [18] R. Alaifari, G. S. Alberti, and T. Gauksson, "Adef: an iterative algorithm to construct adversarial deformations," *arXiv preprint arXiv:1804.07729*, 2018.
- [19] L. Engstrom, B. Tran, D. Tsipras, L. Schmidt, and A. Madry, "A rotation and a translation suffice: Fooling cnns with simple transformations," 2018.
- [20] Y. Song, R. Shu, N. Kushman, and S. Ermon, "Constructing unrestricted adversarial examples with generative models," *arXiv preprint arXiv:1805.07894*, 2018.
- [21] C. Xiao, J.-Y. Zhu, B. Li, W. He, M. Liu, and D. Song, "Spatially transformed adversarial examples," *arXiv preprint arXiv:1801.02612*, 2018.
- [22] C. Guo, M. Rana, M. Cisse, and L. Van Der Maaten, "Countering adversarial images using input transformations," *arXiv preprint arXiv:1711.00117*, 2017.
- [23] C. Kou, H. K. Lee, E.-C. Chang, and T. K. Ng, "Enhancing transformation-based defenses against adversarial attacks with a distribution classifier," in *International Conference on Learning Representations*, 2019.
- [24] W. Xu, D. Evans, and Y. Qi, "Feature squeezing: Detecting adversarial examples in deep neural networks," *arXiv preprint arXiv:1704.01155*, 2017.
- [25] A. Ross and F. Doshi-Velez, "Improving the adversarial robustness and interpretability of deep neural networks by regularizing their input gradients," in *Proceedings of the AAAI Conference on Artificial Intelligence*, vol. 32, no. 1, 2018.
- [26] P. Xia and B. Li, "Improving resistance to adversarial deformations by regularizing gradients," *Neurocomputing*, vol. 455, pp. 38–46, 2021.
- [27] A. Shafahi, M. Najibi, A. Ghiasi, Z. Xu, J. Dickerson, C. Studer, L. S. Davis, G. Taylor, and T. Goldstein, "Adversarial training for free!" *arXiv preprint arXiv:1904.12843*, 2019.
- [28] D. Zhang, T. Zhang, Y. Lu, Z. Zhu, and B. Dong, "You only propagate once: Accelerating adversarial training via maximal principle," *arXiv preprint arXiv:1905.00877*, 2019.
- [29] F. Tramèr, A. Kurakin, N. Papernot, I. Goodfellow, D. Boneh, and P. McDaniel, "Ensemble adversarial training: Attacks and defenses," *arXiv preprint arXiv:1705.07204*, 2017.
- [30] F. Tramèr and D. Boneh, "Adversarial training and robustness for multiple perturbations," *arXiv preprint arXiv:1904.13000*, 2019.

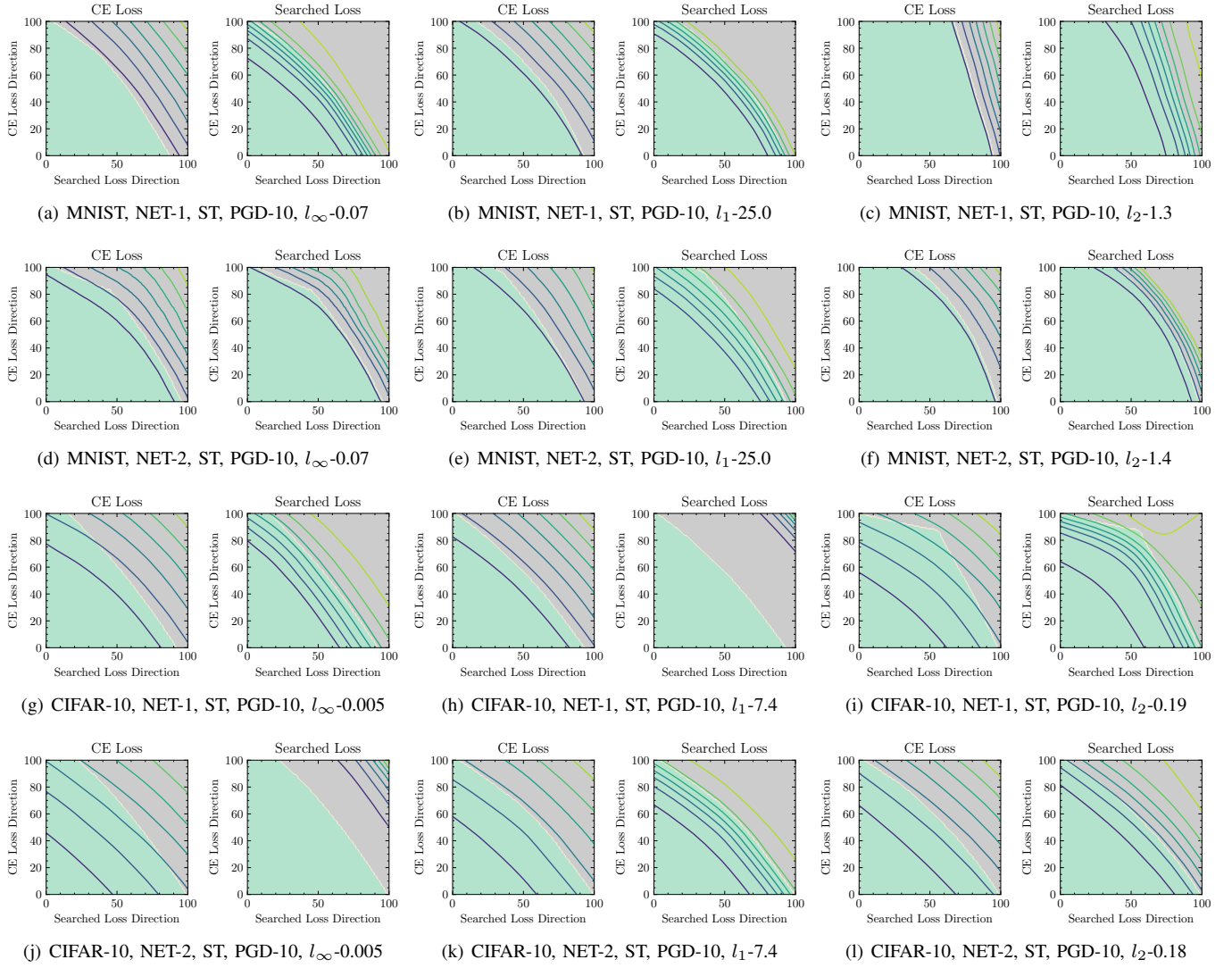


Fig. 9. Local loss landscape on MNIST and CIFAR-10. The vertical axis represents the direction when using the CE loss to generate an adversary. The horizontal axis represents the direction when using the searched loss to generate an adversary. The green area represents $\ell_{0-1} = 0$, the gray area represents $\ell_{0-1} = 1$, and the lines represent the contours of the CE loss or the searched loss.

- [31] J. Wang and H. Zhang, “Bilateral adversarial training: Towards fast training of more robust models against adversarial attacks,” in *Proceedings of the IEEE/CVF International Conference on Computer Vision*, 2019, pp. 6629–6638.
- [32] H. Zhang, Y. Yu, J. Jiao, E. Xing, L. El Ghaoui, and M. Jordan, “Theoretically principled trade-off between robustness and accuracy,” in *International Conference on Machine Learning*. PMLR, 2019, pp. 7472–7482.
- [33] A. Fawzi, O. Fawzi, and P. Frossard, “Analysis of classifiers’ robustness to adversarial perturbations,” *Machine Learning*, vol. 107, no. 3, pp. 481–508, 2018.
- [34] L. Weng, H. Zhang, H. Chen, Z. Song, C.-J. Hsieh, L. Daniel, D. Boning, and I. Dhillon, “Towards fast computation of certified robustness for relu networks,” in *International Conference on Machine Learning*. PMLR, 2018, pp. 5276–5285.
- [35] D. Hendrycks and T. Dietterich, “Benchmarking neural network robustness to common corruptions and perturbations,” *arXiv preprint arXiv:1903.12261*, 2019.
- [36] N. Papernot, P. McDaniel, I. Goodfellow, S. Jha, Z. B. Celik, and A. Swami, “Practical black-box attacks against machine learning,” in *Proceedings of the 2017 ACM on Asia conference on computer and communications security*, 2017, pp. 506–519.
- [37] A. Athalye, N. Carlini, and D. Wagner, “Obfuscated gradients give a false sense of security: Circumventing defenses to adversarial examples,” in *International conference on machine learning*. PMLR, 2018, pp. 274–283.
- [38] B. Zoph and Q. V. Le, “Neural architecture search with reinforcement learning,” *arXiv preprint arXiv:1611.01578*, 2016.
- [39] X. He, K. Zhao, and X. Chu, “Automl: A survey of the state-of-the-art,” *Knowledge-Based Systems*, vol. 212, p. 106622, 2021.
- [40] C. Li, X. Yuan, C. Lin, M. Guo, W. Wu, J. Yan, and W. Ouyang, “Am-lfs: Automl for loss function search,” in *Proceedings of the IEEE/CVF International Conference on Computer Vision*, 2019, pp. 8410–8419.
- [41] X. Wang, S. Wang, C. Chi, S. Zhang, and T. Mei, “Loss function search for face recognition,” in *International Conference on Machine Learning*. PMLR, 2020, pp. 10 029–10 038.
- [42] H. Li, C. Tao, X. Zhu, X. Wang, G. Huang, and J. Dai, “Auto seg-loss: Searching metric surrogates for semantic segmentation,” *arXiv preprint arXiv:2010.07930*, 2020.
- [43] P. Liu, G. Zhang, B. Wang, H. Xu, X. Liang, Y. Jiang, and Z. Li, “Loss function discovery for object detection via convergence-simulation driven search,” *arXiv preprint arXiv:2102.04700*, 2021.
- [44] H. Li, T. Fu, J. Dai, H. Li, G. Huang, and X. Zhu, “Autoloss-zero: Searching loss functions from scratch for generic tasks,” *arXiv preprint arXiv:2103.14026*, 2021.
- [45] P. L. Bartlett, M. I. Jordan, and J. D. McAuliffe, “Convexity, classification, and risk bounds,” *Journal of the American Statistical Association*, vol. 101, no. 473, pp. 138–156, 2006.

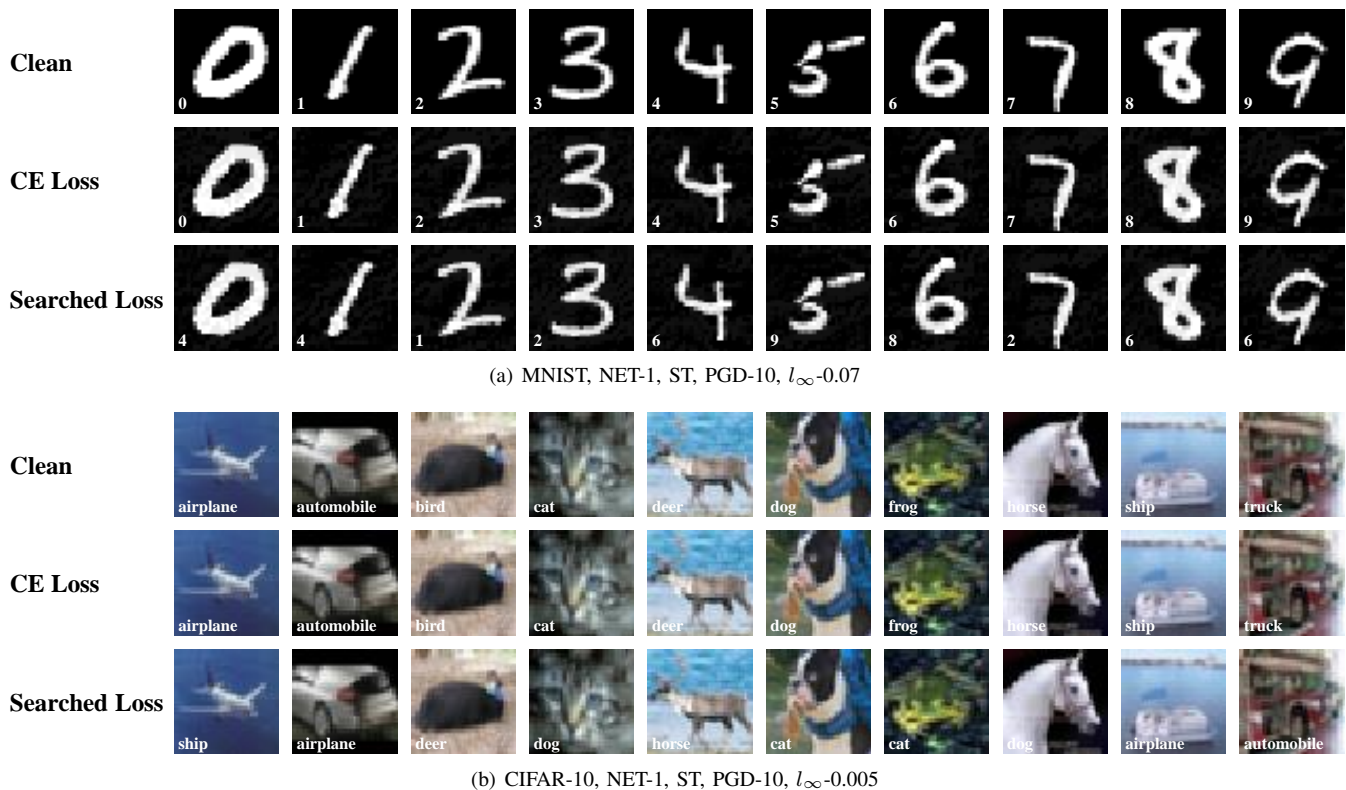


Fig. 10. Qualitative examples of adversarial examples generated with the CE loss and the searched loss.

- [46] A. Tewari and P. L. Bartlett, "On the consistency of multiclass classification methods." *Journal of Machine Learning Research*, vol. 8, no. 5, 2007.
- [47] J. Uesato, B. O'donoghue, P. Kohli, and A. Oord, "Adversarial risk and the dangers of evaluating against weak attacks," in *International Conference on Machine Learning*. PMLR, 2018, pp. 5025–5034.
- [48] F. Croce and M. Hein, "Reliable evaluation of adversarial robustness with an ensemble of diverse parameter-free attacks," in *International conference on machine learning*. PMLR, 2020, pp. 2206–2216.
- [49] D. E. Goldberg and K. Deb, "A comparative analysis of selection schemes used in genetic algorithms," in *Foundations of genetic algorithms*. Elsevier, 1991, vol. 1, pp. 69–93.
- [50] Y. LeCun, L. Bottou, Y. Bengio, and P. Haffner, "Gradient-based learning applied to document recognition," *Proceedings of the IEEE*, vol. 86, no. 11, pp. 2278–2324, 1998.
- [51] A. Krizhevsky, G. Hinton *et al.*, "Learning multiple layers of features from tiny images," 2009.
- [52] C. Yadav and L. Bottou, "Cold case: The lost mnist digits," *arXiv preprint arXiv:1905.10498*, 2019.
- [53] S. Ioffe and C. Szegedy, "Batch normalization: Accelerating deep network training by reducing internal covariate shift," in *International conference on machine learning*. PMLR, 2015, pp. 448–456.
- [54] M. Lin, Q. Chen, and S. Yan, "Network in network," *arXiv preprint arXiv:1312.4400*, 2013.
- [55] A. Paszke, S. Gross, S. Chintala, G. Chanan, E. Yang, Z. DeVito, Z. Lin, A. Desmaison, L. Antiga, and A. Lerer, "Automatic differentiation in pytorch," 2017.
- [56] F.-M. De Rainville, F.-A. Fortin, M.-A. Gardner, M. Parizeau, and C. Gagné, "Deap: A python framework for evolutionary algorithms," in *Proceedings of the 14th annual conference companion on Genetic and evolutionary computation*, 2012, pp. 85–92.